



The Geographic Base

Journal Homepage: <https://www.ngssnepal.org/journal>



Soil Erosion Estimation Using Geospatial Technology: A Study of Jyadul Khola Basin, Gorkha, Nepal

Sandeep Adhikari ^{1,*}, Prabesh Shrestha ², Motilal Ghimire ¹

¹ Central Department of Geography, Tribhuvan University, Kathmandu 44619, Nepal

² Geographical Information Science and System, University of Salzburg, Austria

* Correspondence E-mail: sandeepadh2050@gmail.com

Article info

Keywords:

ERDAS imagine

RUSLE

Kappa coefficient

Erosion severity

Received: 15th Aug. 2022

Accepted: 25th Nov. 2022

DOI: <https://doi.org/10.3126/tgb.v9i1.55436>

© The Geographic Base

Abstract

Estimation of soil erosion from drainage basins is essential while assessing the severity and its impact on agriculture, forests, barren land, waterbodies, and built-up areas. Jyadul Khola basin significantly affects the ecological processes that feed into the Budhigandaki River in the south-eastern side of Gorkha District. This paper has attempted to estimate the mean erosion rate based on the erosion severity classes. Remotely sensed Ziyuan-3 satellite image processed in Earth Resources Data Analysis System (ERDAS) Imagine, Geographical Information System (GIS), and Revised Universal Soil Loss Equation (RUSLE) model were used in this study. The land use land cover (LULC) classification results were validated by using confusion matrix by computing overall accuracy and kappa coefficient which is 95% and 0.94 respectively. The basin had been classified into 6 categories based on erosion severity. The results indicated 92.7% of land ($0-5 \text{ t ha}^{-1} \text{ yr}^{-1}$) is low severe followed by 2.39% ($10-20 \text{ t ha}^{-1} \text{ yr}^{-1}$) moderate, 2.07% ($5-10 \text{ t ha}^{-1} \text{ yr}^{-1}$) high, 2.04% ($20-40 \text{ t ha}^{-1} \text{ yr}^{-1}$) very high, 0.67% ($40-80 \text{ t ha}^{-1} \text{ yr}^{-1}$) severe and 0.10% of land

($>80 \text{ t ha}^{-1} \text{ yr}^{-1}$) which is very severe for soil erosion. The total annual mean soil loss was found to be $13526.60 \text{ t yr}^{-1}$ and soil erosion classes ranges from 0 to $305.34 \text{ t ha}^{-1} \text{ yr}^{-1}$ for the entire study area. Kuwapani, Lakuri Bhanjyang, Khadkagaun, Garapani and Kaulebhar area are the most susceptible to soil erosion. It is observed that barren land, steep slopes, and high intensity of rainfall are major factors for soil erosion hazard. This outcome can serve as a foundation for decision-makers to conserve high risk areas and plan effective measure to lessen impending disasters.

Introduction

Soil erosion is a natural process that is accelerated by anthropogenic activities and natural conditions (Pimentel, 2006). Soil erosion has recently been accelerated by anthropogenic activities such as mining, deforestation, construction, agricultural pesticides, agricultural practices on marginal lands and steep terrain, overstocking and excessive grazing, etc., (Gautam et al., 2013; Negasi et al., 2018; Singh et al., 2016). Natural erosion is caused by the process of topsoil dissociation, transport, and eventually depositing in the presence of high rainfall and strong winds (Jain et al., 2001; Sahu et al., 2017). Soil erosion caused by this mechanism accumulates as sediment in water bodies, lowering the quality of water and carrying capacity of rivers and streams. In the long run, it has a negative impact on the ecology of aquatic areas as well as the shape of

existing rivers. Soil erosion in hilly region is primarily influenced by steep slope, rainfall intensity, soil characteristics, land use and land cover are all factors that encourage significant surface runoff with huge sediments (Nehai et al., 2020). According to studies, climate change directly influences the rate of soil erosion by modifying the pattern of precipitation and temperature, as well as the area's land use, rate of infiltration, biomass yield, surface runoff, and moisture content of soil (Li et al., 2016; Nearing et al., 2004).

Koirala, Thakuri, Joshi and Chauhan (2019) found that the Terai region has the lowest mean annual erosion ($0.1 \text{ t ha}^{-1} \text{ yr}^{-1}$), whereas the Middle Mountain region have the highest potential for erosion ($38.39 \text{ t ha}^{-1} \text{ yr}^{-1}$). The Karnali River basin experienced the greatest annual erosion in million tonnes is (135.8 mT), accompanied by the Gandaki (96.1 mT), Koshi (79.7 mT), Mahakali (15.6 mT) and 2.2 mT for Churiya basin (Koirala et al., 2019). The steepest slopes ($>26.8\%$) showed the highest erosion rates. In Nepal, the water erodes roughly 45.5% of the steeper slopes, mainly due to the wind effect from south or southwest of the country that brings heavy rainfall (Chalise et al., 2019). Typically, cultivated areas experience greater soil erosion than uncultivated areas (Brown, 1984). Since large population practices a poor agricultural mechanism in order to maximizing the yields from available arable land which eventually leads to soil salinity and alkalinity. Overuse

of pesticides and chemical fertilizers, demanding for fuelwood, practices of land fragmentation, over-tilling and monocropping that affect production of food, negative impact on biodiversity and the ability to withstand disasters. Nepal will have to deal with the most difficulties if best farming technologies and suitable land regulations are not implemented.

The systematic management of water resources, soils and vegetations on a drainage basin is crucial to prevent soil erosion and excessive siltation in riverine, lake area, and estuaries. The Revised Universal Soil Loss Equation (RUSLE) has been adapted in the study which is an updated version of the USLE model by Smith and Wischmeier (1978). RUSLE equation improved on better calculations of slope factor and corrected to rainfall runoff erosivity factor. Thus, objectives of this study are to estimate and investigate the impact of six factors; rainfall erosivity, rainfall erosivity, topographic, cover management, support practice and soil loss rate of the Jyadul Khola basin by the help of GIS platform. In order to accomplish the mentioned objectives, the scope of this study comprises image processing in ERDAS imagine, statistical accuracy assessment of Ziyuan-3 satellite image and mapping six factors or components of RUSLE model.

Methods and Materials

The Jyadul is an Urdu name for *Maha-Nadi*, which was granted to Muslims of

Gorkha by King Prithvi Narayan Shah during the Chaubise Rajya of west Nepal. Jyadul river basin occupies portion of Gorkha Municipality, Sahid Laxan and Bhimsen Thapa Rural Municipality of Gorkha District (Figure 1). Its geographic extent is 27° 56' 12" to 28° 1' 46.91" north and 84° 38' 0.85" to 84° 44' 44.79" east. The basin with an area of 66.04 km² rises from 375.28 m to 1500.82 m above mean sea level lies under middle mountainous region. The Jyadul Khola is one of the major tributaries of the Budhi Gandaki River which of catchment area for Trishuli River. The total length of the Jyadul Khola from the first order stream or source point to outlet point or pour point is about 18 km and its basin length is about 12.5 km. As per the geological map the formation of basin area is Ranimatta characterized by grey to greenish grey shales shaly phyllites, slates garnetiferous phyllites, greyish white quartzites with carbonate beds and amphibolite (DMG, 2020). The sal forest is dominant forest type followed by tropical mixed hardwood, lower mixed hardwood, acacia catechu, dalbergia sisso, quercus and pinus roxburghii respectively (DFRS, 2015). Agricultural land characterized by level terraces khet land and slopping terraces that mainly includes maize, rice, wheat and millet cultivation (TSLUMD, 2020). Flood and landslides have long been significant water-induced risks to people's safety and other means of livelihood around Jyadul basin (Gotame & Koirala, 2014).

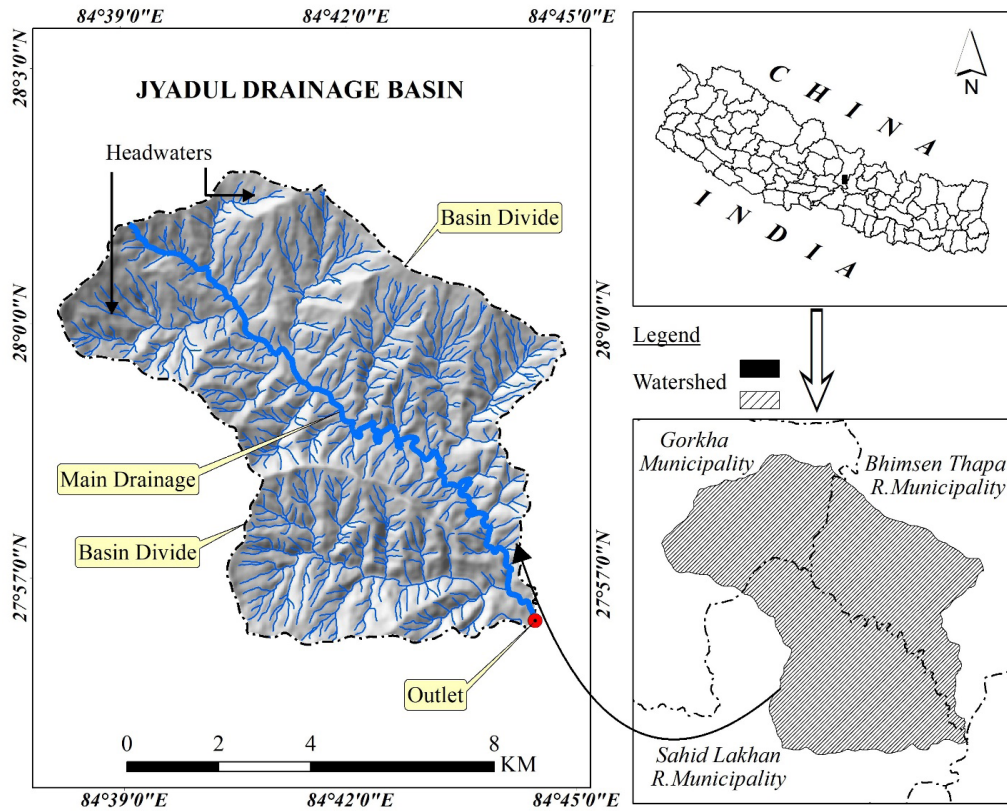


Figure 1. Location of study area

The study was based on quantitative research approach for the statistical analysis of numerical data in order to answer questions such as how much, what, where, when, how many, and how (Apuke, 2017). Rainfall data for the period of 1990 to 2020 was extracted from the power data access supported by National Aeronautics and Space Administration (NASA) (<https://power.larc.nasa.gov/data-access-viewer>). The Ziyuan-3 cloud-free satellite image and digital soil data for the year 2020 were obtained from Topographical Survey and Land

Use Management Division (TSLUMD), Survey Department, Nepal. The image processing was performed in ERDAS Imagine software to achieve a higher level of accuracy. The ERDAS Imagine is a simple and practical software for visualizing and manipulating geographic imaging data (Everitt et al., 1986). Firstly, the images were radiometrically corrected with a particular emphasis on haze and sun angle correction. After the application of radiometric correction, we applied the geometric correction to recompense for errors caused due to

variation in altitude, sensor velocity, earth's rotation and earth curvature etc. In order to improve the geometric accuracy, the rational polynomial coefficient (RPC) were corrected using

ground control points (GCP) obtained from the Differential Global Positioning System (DGPS) survey report of Gorkha and Dhading district provided from TSLUMD.

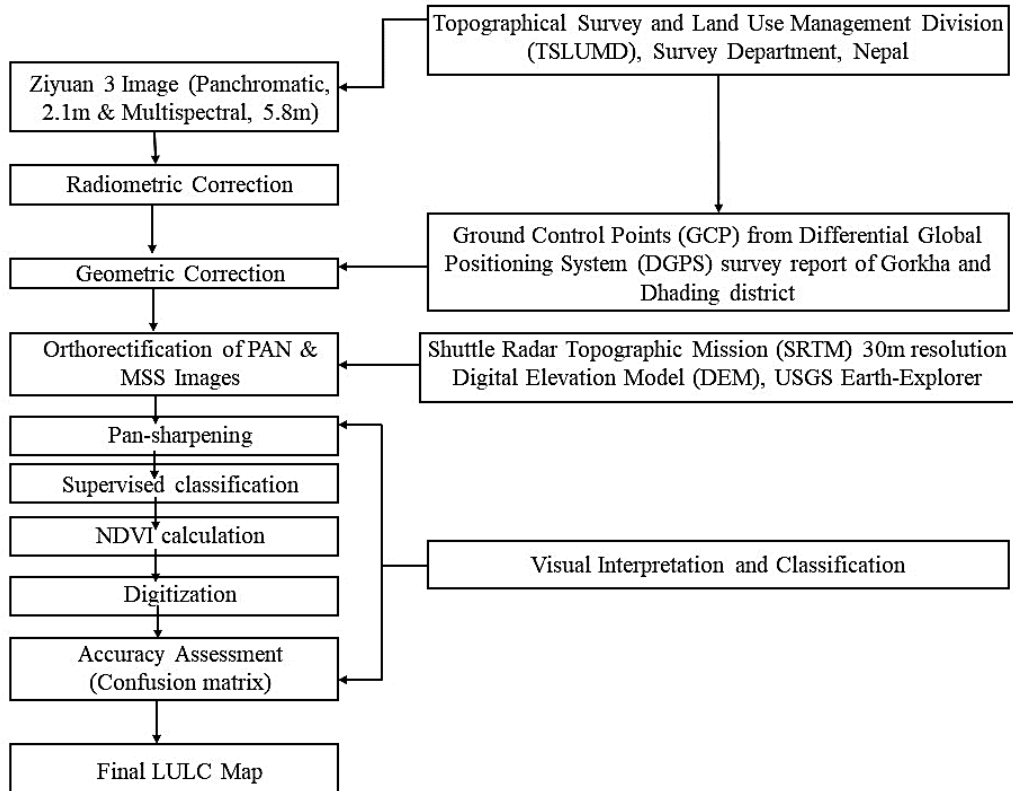


Figure 2. Methodological flow chart of the image processing

The orthorectified image was subsequently prepared in order to represent earth planimetric features or objects as a map by removing the effects of image perspective (tilt) and relief as terrain distortion (Toutin, 2004).

These distortions are eliminated by using Shuttle Radar Topographic Mission (SRTM) 30m resolution Digital

Elevation Model (DEM) extracted from USGS Earth-Explorer (EE) tool. Eventually, pan-sharpening technique (Figure 3) was performed to combine ortho rectified panchromatic image of high spatial resolution (2.1 m) with multispectral image of lower spatial resolution (5.8m). The Nepalese coordinate system of central meridian 84° E of spheroid called Everest 1830 was used

for the two-dimensional representation of the study area as it lies in Gorkha district. Land use land cover (LULC) classification was prepared by applying supervised classification method adopting the maximum likelihood classifier algorithm and digitization technique. The Normalized difference vegetation index (NDVI) calculation was carried for red and near infrared multispectral band. Since spectral information-based classification produces mixed results, it was deemed

unsuitable to directly use as the basis for land use and land cover mapping. Error matrix was created to determine the degree of the error in classification. Subjective judgement was always crucial over this outcome (Figure 2). GIS is a potent set of tools for gathering, storing, retrieving, transforming, and displaying spatial data from the real world, according to Burrough (1986). The drainage basin was delineated in ArcGIS using flow direction raster using hydrology tool.

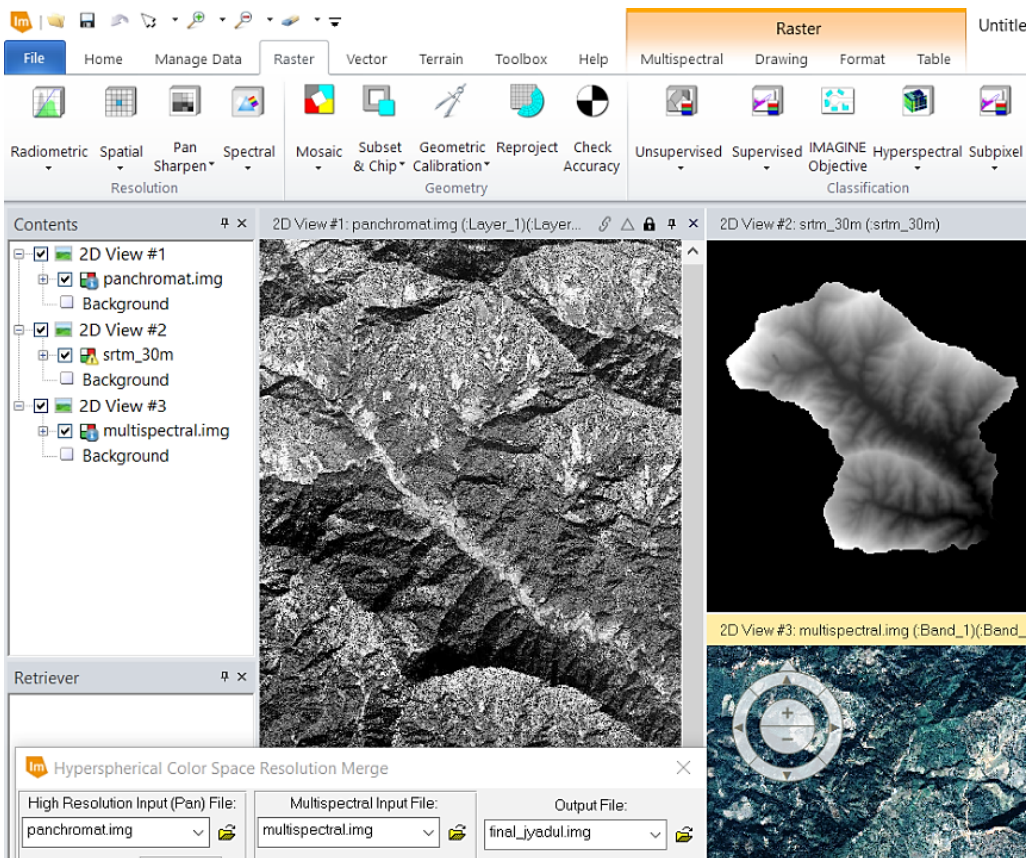


Figure 3. Part of image processing in ERDAS Imagine

Accuracy assessment

Accuracy assessment measures the agreement between a standard presumed to be correct and classified image of uncertain quality. For information extraction by image analysis, accuracy validation is an important step because it establishes the data's worth to the user. (Abubaker et al., 2013). This study used a set of 100 sample points that were randomly placed according to a strategy (Figure 4). ArcMap tools (create random points and spatial join) were applied to distinguish and extract values of five different classes: agricultural land, forest cover, built-up area, waterbodies and barren land. Then, the image of Google Earth was used to figure out what each random point worth. The estimation of Kappa coefficient (Khat Statistics) was computed with the following formula (Congalton, 1991; Rwanga & Ndambuki, 2017).

$$K = \frac{N \sum_{i=1}^r X_{ii} - \sum_{i=1}^r (X_{i+} * X_{+i})}{N^2 - \sum_{i=1}^r (X_{i+} * X_{+i})}$$

Where:

r = number of rows in the matrix

X_{ii} = number of observations in rows i and column I (along the major diagonal)

X_{i+} = marginal total of row i (right of the matrix)

X_{+i} = marginal totals of column i (bottom of the matrix)

N = total number of observations

User's accuracy indicates the probability of an unknown point on the map of being correctly mapped. It measures the

error of commission (error of inclusion). Where; User accuracy = 100% - error of commission. Similarly, Producer's accuracy denotes the probability of an unknown point in the field of being correctly mapped. It measures the error of omission (error of exclusion), where; producer accuracy = 100% - error of omission. The Kappa result be interpreted as: values < 0 as indicating poor, 0.00–0.20 as slight, 0.21–0.40 as fair, 0.41– 0.60 as moderate, 0.61–0.80 as substantial, and 0.81–1.00 as almost perfect agreement (Landis & Koch, 1977; Rwanga & Ndambuki, 2017).

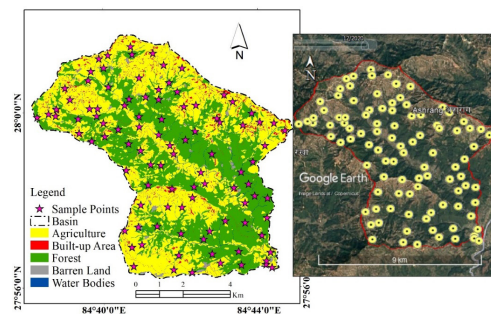


Figure 4. Distribution of sample points in ArcGIS & Google Earth

RUSLE model

It is an empirical model to estimate and predict average annual soil erosion rates by water-induced erosion for agriculture, conservation, mining, construction and forestry uses (Renard et al., 1997). The limitation of RUSLE model is that it is only applicable for estimating rill and sheet erosion; it cannot evaluate the rate of gully erosion and dispersive soils (Thapa, 2020; Rowland, 2019; Wang et al., 2002). Each element was figured out in raster datatype, and the soil erosion

was figured out using map algebra functions in ArcGIS. Figure 5 shows the framework for calculating the RUSLE model, and equation I represents the RUSLE equation,

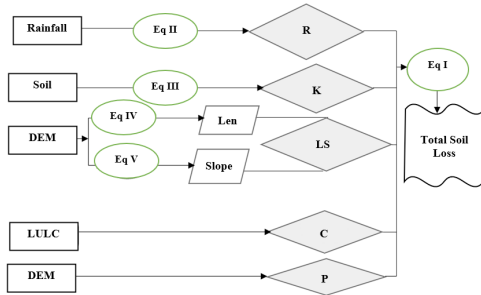


Figure 5. Methodological framework for RUSLE Model

$$A=[R] * [K] * [LS] * [C] * [P],.... \text{ (Eq I)}$$

Here, A is total soil loss in $t \text{ ha}^{-1} \text{ yr}^{-1}$, R is rainfall erosivity ($\text{MJ mm ha}^{-1} \text{ h}^{-1} \text{ yr}^{-1}$), K is soil erodibility factor ($t \text{ h MJ}^{-1} \text{ mm}^{-1}$), LS denotes Slope length steepness factor which is dimensionless, C denotes land management factor which is dimensionless, and P denotes conservation practice factor which is dimensionless.

Rainfall erosivity factor (R)

This rainfall erosion factor (R) interprets the intensity of precipitation at a specific location based on the quantity of rainfall and impacts on soil erosion. It is essential for estimating and predicting soil erosion risk due to climate change and impacts on land use (Stocking, 1984). It quantifies the impact of rainfall amount and runoff rate which is expressed in $\text{MJ mm ha}^{-1} \text{ h}^{-1} \text{ yr}^{-1}$. In the present study, annual rainfall data from 1990 to 2020 was

produced from power data open access supported by National Aeronautics and Space Administration (NASA). The map was prepared using inverse distance weighted (IDW) interpolation using a set of spatially distributed average annual precipitation (P) values in the study area. Rainfall erosivity factor is calculated from the raster calculator in map algebra. The calculation was done using the given equation (Thapa, 2020; Dahal, 2020; Koirala et al., 2019; Morgan et al., 1984).

$$R= 38.5+0.35P..... \text{ (Eq II)}$$

where R=rainfall erosivity factor in $\text{MJ mm ha}^{-1} \text{ h}^{-1} \text{ yr}^{-1}$, P=mean annual rainfall in mm

Soil erodibility factor (K)

The soil erodibility factor (K) describes which types of soil and soil particles are most likely to break apart and be carried away by rain and surface runoff. The K factor is depends on texture of soil, organic matter, soil’s structure, and how well it lets water through. The soil data (Table 1) such as sand%, silt%, clay%, organic content% and soil texture was extracted from digital soil database provided by Topographical Survey and Land Use Management Division (TSLUMD), survey department, Nepal. Those soil data were obtained from detailed field soil survey 2020 and systematic examination in the laboratory by TSLUMD. The calculation was done in Microsoft Excel using the equation provided by Koirala et al. (2019) and Wischmeier & Smith (1978).

$K = Fcsand * Fsi-cl * Forge * Fhisand * 0.1317.....$ (Eq III)

$$Fcsand = \left[0.2 + 0.3 \exp \left(-0.0256 SAN \left(1 - \frac{SIL}{100} \right) \right) \right]$$

$$Fsi-cl = \left[\frac{SIL}{CLA + SIL} \right]^{0.3}$$

$$Forge = 1 - \left[\frac{0.25 ORG}{ORG + \exp(3.72 - 2.95 ORG)} \right]$$

$$Fhisand = 1 - \left[\frac{0.70 \left(1 - \frac{SAN}{100} \right)}{\left(1 - \frac{SAN}{100} \right) + \exp(-5.51 + 22.9 \left(1 - \frac{SAN}{100} \right))} \right]$$

Where, CLA, SIL, SAN, and ORG represents % clay, silt, sand, and organic

carbon content respectively. ‘Fcsand’ is a notation for soil’s low erodibility factor which has coarse sand and high erodibility value with little sand content, ‘Fsi-cl’ stands for low erodibility factor having high clay to silt ratio, ‘Forge’ influenced for the reduction of soil’s erodibility having high organic content, and ‘Fhisand’ influenced for the reduction of soil’s erodibility having sand content high. Later on, soil erodibility map was prepared in ArcGIS with the help of conversion tool for vector to raster.

Table 1. Soil particles in percentage

S. N	Soil Order	Soil Texture	Sand % Topsoil	Silt % Topsoil	Clay % Topsoil	OC % Topsoil
1	Entisols	Sandy Clay Loam	56.4	19.6	24	1.95
2	Entisols	Loam	46.3	45.7	8	2.04
3	Entisols	Loam	36.3	37.7	26	2.81
4	Entisols	Loam	48.8	39.6	11.5	1.84
5	Entisols	Loamy Sand	80.8	13.6	5.5	3.32
6	Entisols	Silty Loam	60.5	31.6	7.8	1.68
7	Entisols	Silty Loam	58.5	29.6	11.8	1.88
8	Inceptisols	Silty Clay	50.8	27.6	21.5	1.34
9	Inceptisols	Loam	42.3	47.7	10	2.13
10	Inceptisols	Silty Clay	8.6	40.4	51	4.74
11	Inceptisols	Loam	46.4	43.6	10	2.48
12	Inceptisols	Silty Loam	40.6	50.4	9	1.31
13	Inceptisols	Sandy Loam	56.4	35.6	8	6.72
14	Inceptisols	Sandy Loam	50.3	47.7	2	3.77
15	Inceptisols	Loam	41.4	42.6	16	2.49
16	Inceptisols	Silty Loam	56.8	31.6	11.5	1.75
17	Inceptisols	Clay	44.7	23.6	31.6	1.21
18	Inceptisols	Loam	46.7	29.6	23.6	3.15
19	Inceptisols	Silty Clay	46.8	25.6	27.5	1.34
20	Inceptisols	Loam	38.3	49.7	12	1.91
21	Inceptisols	Sandy Loam	48.3	46.2	5.5	1.61
22	Inceptisols	Clay Loam	24.4	37.6	38	1.31
23	Inceptisols	Silty Loam	60.8	27.6	11.5	2.68

Source: TSLUMD, 2020

Topographic factor (LS)

The topographic factor is influenced by slope length (L) and the slope steepness (S). The slope-length factor is a key parameter for modeling soil erosion and figuring out how much surface runoff can move. When the slope length of a particular area increases then soil loss or erosion increases in steep slope (Ganasri & Ramesh, 2016). The soil loss depends on the size of soil particle and how much vegetation there is in a particular area. The LS factor denotes the topographical effect mainly the steepness and slope length of hilly region. Shuttle Radar Topographic Mission (SRTM) dem of 30 m resolution was acquired and spatial analyst tools (sink, fill, flow direction and slope) were used to analyze and evaluate in Arc GIS environment (Adhikari, 2020). The product of slope length and the slope steepness factor was calculated in the topographical factor grid using the given equation (Thapa, 2020; Koirala et al., 2019; Atoma, 2018).

$$L = \left(\frac{\lambda}{22.13} \right)^m$$

where, L is slope length factor, λ is slope length in meter, m is slope-length exponent

$$m = \frac{F}{1 + F}$$

$$F = \frac{\frac{\sin \beta}{0.0896}}{3(\sin \beta)^{0.8} + 0.56}$$

where, F = ratio of rill erosion to inter-rill erosion, β = slope angle in degree

Then, the calculations were done in ArcGIS using raster calculator tool.

For, Slope length factor ‘L’ (Eq IV);

$$L = \left(\frac{(\text{Flow Acc} + 625)^{(m+1)}}{25^{(m+2)} * 22.13^{(m)}} - \frac{\text{Flow Acc}^{(m+1)}}{25^{(m+2)} * 22.13^{(m)}} \right)$$

Similarly, slope gradient factor (S);

$$S = \text{Con} ((\text{Tan} (\text{slope} * 0.01745) < 0.09), (10.8 * \text{Sin} (\text{slope} * 0.01745) + 0.03),$$

$$(16.8 * \text{Sin} (\text{slope} * 0.01745) - 0.5)), \dots \dots \dots (\text{Eq V})$$

Final, LS factor = L * S

Cover management factor (C)

The C-factor takes into account how different Land Use / Land Cover (LULC) affect soil erosion such as forest, cultivation, water bodies, snowy glacier, grassland, shrubland, built-up areas, barren land and so on. The C-factors play a vital role in crop management. Vegetation cover is crucial in controlling the risk of soil erosion by improving water holding capacity, delaying and reducing surface water runoff, preventing soil surface from raindrop splashing, control sheet erosion, lessen rainfall energy by increasing interception and infiltration rate. The study was classified in five land categories (Table 2) where C factor value for each LULC assigned according to Thapa (2020) & Panagos et al. (2015). The C values ranges from 0 to 1 where lower C denotes minimum soil loss with very strong coverage, while higher C means uncover surface and higher possibility for loss of soil.

Table 2. Cover Management Factor (C)

Land use land cover	C-factor
Forest and Shrubland	0.03
Agricultural land	0.21
Barren land	0.45
Water Body	0
Built-up Area	0

Source: Thapa, (2020)

Support practice factor (P)

It expresses the soil loss based on the different cultivated lands. Contouring, cropping, and terraces are some of the measures used to control soil erosion. The P values vary from 0 to 1 where 0 indicates a very good anthropogenic erosion resistance and 1 denotes a facility without anthropogenic resistance to erosion (Kouli et al., 2009). Based on Nepal's physiography, Land Resource and Mapping Project (LRMP) has widely classified cultivated land into tarai, hill, mountain, and valley farming. The study area lies in hilly region which consist of level and slopping terrace farming practices. As a method of conservation farming or agricultural support practice, terrace construction almost resembles contour farming. In this study, values were assigned as per contouring method (Koirala et al., 2019). The slope percentage was reclassified as per the value (Table 3) then converted to raster in ArcGIS.

Table 3. Cover Management Factor (C)

Slope %	Contouring (P)
0 – 7	0.55
7 - 11.3	0.6
11.3 - 17.6	0.8
17.6 - 26.8	0.95
> 26.8	1

Source: Koirala et al., (2019)

Results and Discussion

Examining the accuracy

In this study, the accuracy agreement between a standard assumed (google earth imagery of 2020) and classified image (Ziyan-3 of 2020) has been inspected and evaluated as per the Landis & Koch (1977) and Rwanga & Ndambuki (2017) interpretation. The calculation is given below;

$$\text{Overall accuracy} = \left(\frac{\text{Sum of diagonal}}{\text{Total number of sample}} \right) * 100\% = \left(\frac{95}{100} \right) * 100\% = 95\%$$

In row, User's Accuracy (%) for agriculture is

$$= \left(\frac{\text{no.of correct in a class}}{\text{no of points in class in the map}} \right) * 100\% = \left(\frac{36}{38} \right) * 100\% = 94.74\%$$

In column, Producer's Accuracy (%) for agriculture is

$$= \left(\frac{\text{no.of correct in a class}}{\text{no of points in class in the map}} \right) * 100\% = \left(\frac{36}{38} \right) * 100\% = 94.74\%$$

The procedure for calculating user accuracy and producer accuracy is similar for other categories in row and column. The calculation for Kappa coefficient (khat statistics) is computed using following equation.

$$\begin{aligned}
 K &= \frac{N \sum_{i=1}^r X_{ii} - \sum_{i=1}^r (X_{i+} * X_{+i})}{N^2 - \sum_{i=1}^r (X_{i+} * X_{+i})} \\
 &= \frac{(9500 - 2212)}{(100^2 - 2212)} \\
 &= 0.94
 \end{aligned}$$

the classified objects (agricultural land, forest coverage, water bodies, built-up area and barren land) of the Jyadul khola basin. So, statistics indicate the agreement is almost perfect which is considered as the closeness of measured value to the truth value (Table 4).

The overall accuracy and kappa coefficient are found 95% and 0.94 respectively for

Table 4. Confusion matrix

		Validation data (Google image)								
		LULC class	Agr	For	Built up	Bare	Water	Total (User)	Commission error	User's accuracy (%)
Classification (Ziyan-3)	Agriculture	36	1		1		38	5.26	94.74	
	Forest	1	26				27	3.70	96.30	
	Built-up				19		19	0.00	100.00	
	Barren	1				5	6	16.67	83.33	
	Water bodies			1			9	10.00	90.00	
	Total (Producer)	38	28	19	6	9	100			
	Omission error	5.26	7.14	0.00	16.67	0.00				
	Producer's accuracy (%)	94.74	92.86	100	83.33	100				
	Overall accuracy (%)								95	
	Kappa coefficient								0.94	

Source: Calculation by author based on formula (Congalton, (1991); Rwanda & Ndambuki, (2017)

Rainfall erosivity factor (R)

The study area lies within a range of 829.29 to 989.87 mm of average rainfall. The outcome shows that the R factor lies between 328.8 to 385 MJ mm ha⁻¹

h⁻¹ yr⁻¹. The northern part of study area as indicated by red color has higher erosivity and south-eastern, southern, south-western part as indicated by blue color has lower erosivity rate (Figure

6). The soil erosion by intensity of precipitation around Labsibot, Pipalthok, Kuwapani, Garapani, Deragaun, Khiprugaun, Khabdigaun, Kumaltar, Tiwarigaun, Hilekharka, Toikepani, Phinam, Baniyagaun, Bahungaun, Aultari, Aruswanra, Luichiswanra, Dhanumase and Bahungaun are higher. Similarly, area around Mohariya, Thamdanda, Thamdanda, Gagatetar, Rukhanthumdanda, Tersegaun, Ripthok, Khandanda, and Chautaradanda have lower erosivity due to precipitation.

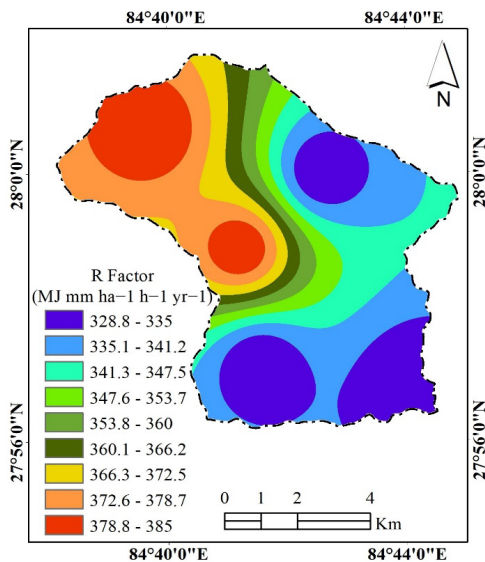


Figure 6. Rainfall erosivity map

Soil erodibility factor (K)

The study shows that K factor values range from 0.0404 to 0.0166 t h MJ⁻¹ mm⁻¹ (Figure 7 & Table 5).

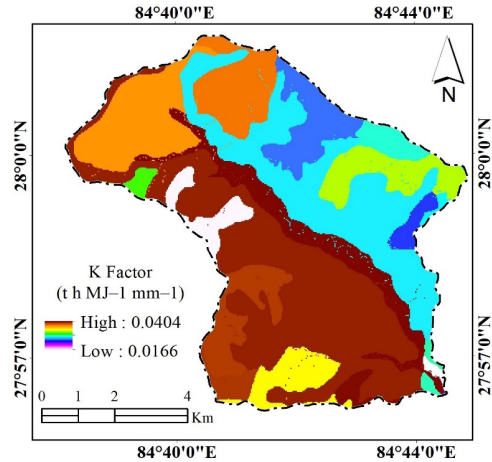


Figure 7. Soil erodibility map

The rate at which soil particles are susceptible to dissociation and transport by rainfall and runoff indicates low in Kyamuntar and high around Bhanthanabesi & Thapatar area. The ability of the soil to hold nutrients and moisture is decreased with decreasing pattern of forest and agricultural land (TSLUMD, 2020). So, rainstorm leads to increased runoff and erosion. Activities such as gully, rill, and stream erosion contribute to the downstream impacts of floods, farms built on steep hillsides and sedimentation caused by eroded soil due to water action, that ultimately increases the sediments. Agriculture lands are highly susceptible to surface soil erosion. The calculated value of K is product of Fcsand, ‘Fsi-cl’, Forge and Fhisand with 0.1317 as shown in Table 5.

Table 5. Calculated value for soil erodibility

S. N	Fcsand	Fsi-cl	Forgc	Fhisand	K factor
1	0.2940	0.7867	0.7657	0.9965	0.0232
2	0.3576	0.9528	0.7617	0.9996	0.0342
3	0.3681	0.8544	0.7509	0.9999	0.0311
4	0.3411	0.9264	0.7724	0.9993	0.0321
5	0.2502	0.9031	0.7502	0.7418	0.0166
6	0.3040	0.9360	0.7869	0.9920	0.0293
7	0.3045	0.9042	0.7697	0.9947	0.0278
8	0.3170	0.8413	0.8429	0.9989	0.0296
9	0.3703	0.9445	0.7587	0.9998	0.0349
10	0.4631	0.7828	0.7500	1.0000	0.0358
11	0.3535	0.9399	0.7527	0.9996	0.0329
12	0.3792	0.9519	0.8495	0.9999	0.0404
13	0.3184	0.9410	0.7500	0.9965	0.0295
14	0.3530	0.9878	0.7500	0.9990	0.0344
15	0.3633	0.9088	0.7526	0.9998	0.0327
16	0.3110	0.9111	0.7797	0.9962	0.0290
17	0.3252	0.7750	0.8725	0.9997	0.0289
18	0.3293	0.8387	0.7503	0.9995	0.0273
19	0.3230	0.8034	0.8429	0.9995	0.0288
20	0.3832	0.9372	0.7679	0.9999	0.0363
21	0.3542	0.9668	0.7954	0.9994	0.0359
22	0.4032	0.8110	0.8495	1.0000	0.0366
23	0.2972	0.9008	0.7514	0.9915	0.0263

Source: Calculation by author based on Eq III

Topographic factor (LS)

The topographic factor map (Figure 8) is the raster product of slope-length factor (L) with slope gradient factor (S). The LS value for this study ranges from 0 to 94.11 which is dimensionless. The white portion indicates highest value that means steepness of ground is high where chances of soil loss per unit area will be more. Similarly, black portion indicates

the gentle and gradual slope which has less chances of soil loss per unit area. The large area is covered by black portion which means low chances of soil loss in overall basin area due to topographic factor. The study area holds major threat of landslide in steep ground along road network and flood alongside the jyadul khola due to topographic condition.

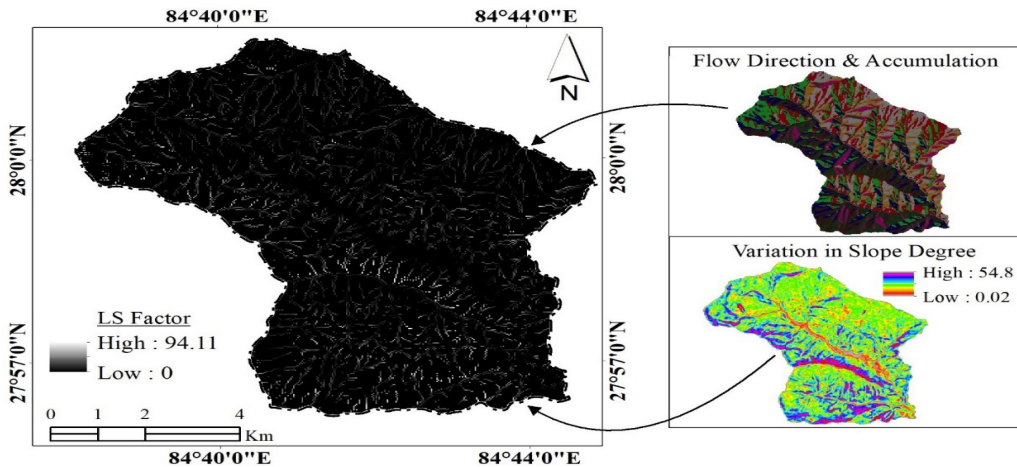


Figure 8. Topographic factor map
Cover management factor (C)

The result shows that C factor values range from 0 to 0.45 (Figure 9). The higher values specify no cover effect, poor crop management practices and significant chances of soil loss which is barren land and open spaces with no trees.

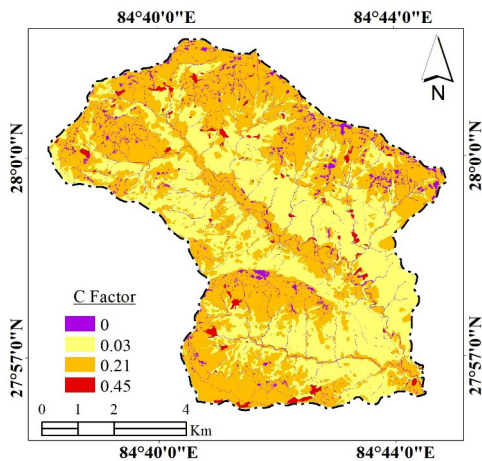


Figure 9. Cover management map

The C value of 0 means a strong cover effect resulting in very few chances of soil erosion due to land cover and land use impact in the study area. Compared with forest, agriculture and barren land, the land cover with concrete (built-up) has less chance of soil loss. In the study area, built-up comprises of residential, commercial, educational, security services, road networks, health services, institution, public area, man-made open area, industry, historical, archeological and religious site. However, forest land degradation reported due to an increasing population that demanded land for cultivation, forest based economic activities such as building materials, construction, furniture, food, fuel, raw materials for industrial processing and household equipment. Additionally, availability of off-farm income in cities, declining agricultural productivity, labor shortages, inadequate returns from traditional farming, foreign labor

migration and geographical proximity to cities have all emerged as the main causes of land abandonment, which has led to the decline of agricultural land and increase in barren land (TSLUMD, 2020).

Support practice factor (P)

The result (Figure 10) shows that the support practice factor (P) values range from 0.55 to 1. It indicates the area with P value 0.55 to 0.95 represents good anthropic erosion resistance facility which is not complicated to construct, extremely dependable, and highly effective in controlling run-off and to prevent soil erosion from the slope. Similarly, P value with 1 indicates a non-anthropogenic resistance erosion facility that means steep slope enhance the number and speed of runoff which ultimately

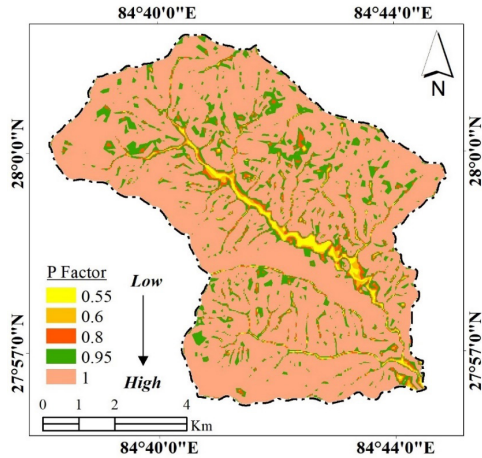


Figure 10. Support practice map

Potential soil erosion (A)

The composite raster map of five factors R, K, LS, C and P were generated by raster calculator tool using the RUSLE relation.

The statistics (Table 6) were calculated using zonal statistics function (spatial analysis tool) on values of a raster cell. In this study, soil erosion ranges from 0 to 305.34 t ha⁻¹ yr⁻¹ and total annual mean soil loss is found to be 13526.60 t yr⁻¹. The annual mean soil erosion for class 20 to 40 that covered 135.30 ha land is found to be higher whereas for class above 80 that covered 6.83 ha out of 6603.87-hectare land has low annual mean soil erosion.

Table 6. Potential rate of soil erosion for study area

Erosion Class (t ha ⁻¹ yr ⁻¹)	Min	Max	Mean Erosion Rate (t ha ⁻¹ yr ⁻¹)	Annual mean soil erosion (t yr ⁻¹)
0 to 5	0.00	5.00	0.17	997.12
5 to 10	5.00	10.00	7.23	1277.79
10 to 20	10.01	19.99	14.49	2757.67
20 to 40	20.00	39.99	27.79	4660.14
40 to 80	40.00	79.96	52.03	2888.97
Above 80	80.43	305.34	107.13	944.91

Source: Calculation in ArcGIS using zonal statistics tool

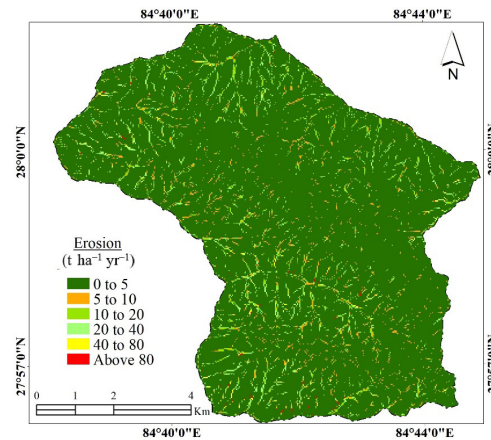


Figure 11. Map depicting potential rate of soil erosion for study area

The entire study area is divided into six erosion classes based on the erosion severity (Table 7 & Figure 11) which is referenced from Koirala et al. (2019). Out of total 6603.87-hectare land, 92.72 % area is low severe, followed by the moderate, severe, high, very high and very severe classes while 1st priority is required in very severe area. It is found that certain area of Kuwapani, Lakuri Bhanjyang, Khadhagaun, Garapani, Hilekharka and Kaulebhar are very severe to potential soil erosion. The haphazard construction of road network, forest-based activities such as construction, furniture & fuel, gradual agricultural land abandonment, degraded & acidic soil by the application of nitrogenous fertilizer like urea, use of enormous amounts of insecticides & pesticides, and intense rainfall in steep slope are the major drivers for soil erosion of the study area. It leads to deposition of pebbles, gravels and sand in the mouth of basin.

Table 7. Soil erosion classes based on severity and importance of conservation

Erosion Rate	Class	Area (ha)	Area (%)	Conservation priority
0 to 5	Low severe	6123.16	92.72	6
5 to 10	Moderate	136.85	2.39	5
10 to 20	High	157.73	2.05	4
20 to 40	Very high	135.30	0.67	3
40 to 80	Severe	44.01	2.07	2
Above 80	Very severe	6.83	0.10	1

Conclusion

This study of Jyadul river basin regarding the assessment of soil erosion have proved to be an effective with the use of GIS, Remote sensing and RUSLE model. The execution of map algebra is possible through raster calculator tool in ArcGIS platform. Based on the qualitative interview and secondary sources, the observed values confirmed that soil erosion is caused by intense rainfall, excessive use of pesticides & fertilizers, haphazard construction of roads and buildings, decline of agricultural land, slope steepness and gradual climate change. The erosion rate for the entire basin is determined to be between 0 to 305.34 t ha⁻¹ yr⁻¹. The study highlights that 7.28% of the area requires attention for conservation to lessen the risk of soil erosion. The sustainable land resource management is required to overcome the problems of deteriorating environmental condition, uncontrolled development and loss of prime agricultural lands.

References

- Abubaker, H. M., Elhag, A.M.H., and Salih, A.M. (2013). Accuracy assessment of land use and land cover classification: Case study of Shomadi area-Renk County-Upper Nile State, South Sudan. *International Journal of Scientific and Research Publications*, Volume 3, Issue 5.
- Adhikari, S. (2020). Morphometric analysis of a drainage basin: A study of Ghatganga River, Bajhang District,

- Nepal. *The Geographic Base*. 7. 127-144. 10.3126/tgb.v7i0.34280.
- Apuke, O. (2017). Quantitative research methods: A synopsis approach. *Arabian Journal of Business and Management Review (kuwait Chapter)*. 6. 40-47. 10.12816/0040336.
- Atoma, H. (2018). Assessment of soil erosion by RUSLE model using remote sensing and GIS techniques: a case study of Huluka Watershed, Central Ethiopia, *PhD Thesis*, Addis Ababa University
- Brown, L. R., & Wolf, E. C. (1984). Soil Erosion: Quiet crisis in the world economy. *Worldwatch Paper* 60.
- Burrough, P.A. (1986). Principles of geographical information systems for land resources assessment. *Oxford University Press*, Oxford.
- Chalise, D., Kumar, L., Spalevic, V., and Skataric, G. (2019). Estimation of sediment yield and maximum outflow using the IntErO model in the Sarada River Basin of Nepal. *Water (Switzerland)*, 11(5). <https://doi.org/10.3390/w11050952>
- Congalton, R.G. (1991). A review of assessing the accuracy of classification of remotely sensed data. *Remote Sensing of Environment*. 37:35-46. [https://doi.org/10.1016/0034-4257\(91\)90048-B](https://doi.org/10.1016/0034-4257(91)90048-B)
- Dahal, R. (2020). Soil erosion estimation using RUSLE modeling and geospatial tool: Case study of Kathmandu District, Nepal. *Forestry Journal of Institute of Forestry*. 17:118-134. <https://doi.org/10.3126/forestry.v17i0.33627>
- DFRS. (2015). *Digital database*. Kathmandu: Department of Forest Research and Survey.
- DMG. (2020). *Geological map of Gorkha District*. Kathmandu: Department of Mines and Geology.
- Everitt, I. H., Richardson, A. J., & Nixon, P. R. (1986). Canopy reflectance characteristics of succulent and nonsucculent rangeland plant species. *Photogrammetric engineering and remote sensing (USA)*. 52:1891-1897.
- Ganasri, B.P., Ramesh. H. (2016). Assessment of soil erosion by RUSLE model using remote sensing and GIS: A case study of Nethravathi Basin. *Geoscience Front*. 7(6):953–961
- Gautam, S.K., Sharma, D., Tripathi, J.K., Ahirwar, S., & Singh, S.K. (2013). A study of the effectiveness of sewage treatment plants in Delhi region. *Applied Water Science*, 3(1), 57-65.
- Gotame, R.P., Koirala, M. (2014). Vulnerability assessment of local people's livelihood in context of water induced hazard: A case study from

- Jyadul khola catchment, Gorkha. *DRM Knowledge Brief*, Issue 1, Yr.1
- Jain, S.K., Kumar, S., & Varghese, J. (2001). Estimation of soil erosion for a Himalayan watershed using GIS technique. *Water Resources Management*, 15(1), 41-54.
- Koirala, P., Thakuri, S., Joshi, S., & Chauhan, R. (2019). Estimation of soil erosion in Nepal using a RUSLE modeling and geospatial tool. *Geosciences (Switzerland)*, 9(4), 1-19.
- Kouli, M., Soupios, P., Vallianatos, F. (2009). Soil erosion prediction using the revised universal soil loss equation (RUSLE) in a GIS framework, Chania, Northwestern Crete, Greece. *Environ Geol* 57(3):483–497. <https://doi.org/10.1007/s00254-008-1318-9>
- Landis, J.R., Koch, G.G. (1977). A one-way components of variance model for categorical data. *Biometrics*. 33, 671-679. <https://doi.org/10.2307/2529465>
- Li, Z., Fang, H. (2016). Impacts of climate change on water erosion: A review, *Earth-Science Reviews*, 163, 94–117. <https://doi.org/10.1016/j.earscirev.2016.10.004>
- Morgan, RPC., Morgan, DDV., Finney, HJ. (1984). A predictive model for the assessment of soil erosion risk. *J Agric Eng Res*. 30:245–253
- Nearing, M.A., Pruski, F.F., O’neal, M.R. (2004). Expected climate change impacts on soil erosion rates: a review. *Journal of Soil and Water Conservation*, 59, 43–50.
- Negasi, S., Hadgu, H., Ted, A., Opoku, P., Isaac, K.A., Emiru, B. (2018). Forest cover change, key drivers, and community perception in Wujig Mahgo Waren forest of northern Ethiopia. *Land* 7(1), 32; <https://doi.org/10.3390/land7010032>
- Nehai, S.A., Guettouche, M.S., & Saadoud, D. (2020). Regional modeling of soil sensitivity to water erosion in JIJEL region (Algeria) using MCA and GIS. *Applied Geomatics*. <https://doi.org/10.1007/s12518-020-00316-5>
- Panagos, P., B., P., Meusburger, K., Alewell, C., Lugato, E., Montanarella, L. (2015). Estimating the soil erosion cover-management factor at the European scale. *Land Use Policy*. 48:38–50
- Pimentel, D. (2006). Soil erosion: A food and environmental threat. *Environment, Development and Sustainability*, 8(1), 119-137
- Renard, K.G., Foster, G., Weesies, G., McCool, D., Yoder, D. (1997). Predicting soil erosion by water: *A guide to conservation planning with the revised universal soil loss equation (RUSLE)*; United

- States Department of Agriculture: Washington, DC, USA, Volume 703.
- Rowlands, L. (2019). Erosion and sediment control - WSUD during the construction phase of land development. *Approaches to Water Sensitive Urban Design*. Chapter 8, 163-176. <https://doi.org/10.1016/B978-0-12-812843-5.00008-3>.
- Rwanga, S., Ndambuki, J.M. (2017). Accuracy assessment of land use land cover classification using remote sensing and GIS. *International Journal of Geosciences*. 8:611–622 (Scientific Research Publishing)
- Sahu, A., Baghel, T., Sinha, M., Ahmad, I., & Verma, M. (2017). Soil erosion modeling using RUSLE and GIS on Dudhawa Catchment. *International Journal of Applied Environmental Sciences*, 12, 1147- 1158.
- Stocking, M. (1984). Rates of erosion and sediment yield in the African environment. *Chall Afr Hydrol Water Resour*, 285–295, IAHS Publ. no. 144.
- Thapa, P. (2020). Spatial estimation of soil erosion using RUSLE modeling: a case study of Dolakha district, Nepal. *Environmental Systems Research*, 9:15. <https://doi.org/10.1186/s40068-020-00177-2>
- Toutin, T. (2004). Geometric processing of remote sensing images: models, algorithms and methods (review paper). *International Journal of Remote Sensing*, 10 pp. 1893-1924
- TSLUMD (2020). *Land use database and reports of gorkha District for the year 2020*. Kathmandu: Topographical Survey and Land Use Management Division, Survey Department, Nepal.
- Wang G., Gertner G., Singh V., Shinkareva S., Parysow P., & Anderson A. (2002). Spatial and temporal prediction and uncertainty of soil loss using the revised universal soil loss equation: a case study of the rainfall–runoff erosivity R factor. *Ecol Model*, 153(1-2):143-155
- Wischmeier, W.H., & Smith, D.D. (1978). Predicting rainfall erosion losses - *A guide to conservation planning*, U.S. Department of Agriculture, Science and Education Administration: Hyattsville, MD, USA, p. 62.